A Contact Algorithm in the Low Velocity Impact Simulation with SPH

Min Oakkey*
Department of Mechanical Design and Production, Yonsei University
Lee Jeongmin
Technical Research Laboratory, Angang Plant, Poongsan Corporation
Kim Kukwon, Lee Sungsoo
Graduate School, Yonsei University

The formulation of Smoothed Particle Hydrodynamics (SPH) and a shortcoming of traditional SPH in contact simulation are presented. A contact algorithm is proposed to treat contact phenomenon between two objects. We describe the boundary of the objects with non-mass artificial particles and set vectors normal to the contact surface. Contact criterion using non-mass particles is established in this study. In order to verify the contact algorithm, an algorithm is implemented in to an in-house program; elastic wave propagation is an analysed under low velocity axial impact of two rods. The results show that the contact algorithm eliminates the undesirable phenomena at the contact surface; numerical result with the contact algorithm is compared with theoretical one.

Key Words : Smoothed Particle Hydrodynamics, Rod Impact, Wave Propagation, No-mass Artificial Particle, Contact Criterion

1. Introduction

Smoothed Particle Hydrodynamics (SPH) is a pure Lagrangian hydrocode and gridless method which employs particles. The method was invented as an alternative to conventional grid-based hydrocodes which have drawbacks such as the grid tangling in Lagrangian technique at large deformation or the increase of computational cost in Eulerian technique at void formation. SPH was introduced by Lucy (1977) for an application in astrophysics and has been developed by many researchers in various fields. The basic concept and formulation were reviewed by Monaghan and Gingold (1977, 1982, 1983). Libersky, et al. (1990, 1993) performed applications of SPH to the analysis of elasto-plastic deformation under high velocity impact. Since SPH is appropriate in the analysis of impact problem involving formation of large deformation and void, the main fields of its application have been in the analyses of the astrophysics, the fluid dynamics and the hypervelocity impact physics.

However, SPH has some significant weaknesses such as the tensile instability confusing the analyses of fracture and fragmentation, and the approximate spatial gradient reducing the accuracy. The potential of SPH is additionally weakened by the lack of boundary conditions which limits the applicability, the instability at the contact surfaces under impact, and the instability at impact between dissimilar materials and with gap.

In the elasto-plastic deformation under low velocity impact, contact conditions affect the analysis considerably whereas the effects of contact conditions can be neglected in case of high velocity impact producing large deformation in

* Corresponding Author,
E-mail : minokey@bubble.yonsei.ac.kr
TEL : +82-2-361-2817 ; **FAX** : +82-2-362-2736
Department of Mechanical Design and Production, Yonsei University, 134, Shinchon-dong, Seodaemun-ku, Seoul 120-749, Korea. (Manuscript **Received** July 24, 1998; **Revised** April 7, 2000)

transient time. In this paper, a review of concept and formulation of SPH is presented with artificial viscosity and artificial heat transfer for treatment of numerical instability. Elastic wave propagation in low velocity longitudinal impact of two rods is analysed with the SPH. Anomalous results at contact surfaces are obtained in the simulation based on the traditional SPH formulation. A contact algorithm is therefore proposed to resolve the undesirable phenomena at the contact surfaces. This algorithm uses non-mass artificial particles located on boundary surface and contact criterion.

2. SPH Equations

The SPH is based on the kernel approximation of field variables and spatial derivatives at randomly distributed points using the kernel function for interpolation. For numerical calculation, the kernel approximation is converted into the particle approximation as a discrete form. The concept of kernel function and approximation are given in Appendix.

2.1 SPH form of governing equations

The governing equations of hydrodynamics consist of continuity equation, momentum conservation equation, and energy conservation equation. The SPH forms of the governing equations can be represented as Eqs. (1) ~ (3) where the variables at a particle i are determined by the variables at particles j.

$$\left(\frac{d\rho}{dt}\right)_i=\left(-\rho\frac{\partial U^\alpha}{\partial x^\alpha}\right)_i$$
$$=-\rho_i\sum_j\frac{m_j}{\rho_i}(U_j^\alpha-U_i^\alpha)\,W_{ij,\alpha(i)} \quad (1)$$
$$\left(\frac{dU^\alpha}{dt}\right)_i=\left(-\frac{1}{\rho}\frac{\partial\sigma^{\alpha\beta}}{\partial x^\beta}\right)_i$$
$$=-\sum_j m_j\left(\frac{\sigma_i^{\alpha\beta}}{\rho_i^2}+\frac{\sigma_j^{\alpha\beta}}{\rho_j^2}\right)W_{ij,\beta(i)} \quad (2)$$
$$\left(\frac{dE}{dt}\right)_i=\left(-\frac{\sigma^{\alpha\beta}}{\rho}\frac{\partial U^\alpha}{\partial x^\beta}\right)_i$$
$$=-\sum_j m_j\frac{\sigma_i^{\alpha\beta}}{\rho_i^2}(U_j^\alpha-U_i^\alpha)\,W_{ij,\beta(i)} \quad (3)$$

Here t, x, ρ, m, U, σ and E are time, position vector, density, mass, velocity vector, total stress tensor and internal energy, respectively. The superscripts α and β are tensor notations which represent the direction in space and $W_{ij,\alpha(i)}$ means the derivative of kernel function W_{ij} of particle i with respect to coordinate x^α.

2.2 Artificial viscosity and artificial heat transfer

In the analysis of impact problem, numerical oscillation occurs at the impact interface where abrupt change in physical variables exist. Artificial viscosity is introduced to reduce the numerical oscillation. Monaghan and Gingold (1983) suggested artificial viscosity Π_{ij} when two particles approach each other as Eq. (4),

$$\Pi_{ij}=\frac{-k_1\overline{c_{ij}}\mu_{ij}+k_2\mu_{ij}^2}{\overline{\rho_{ij}}}, \quad (4)$$

where $\overline{c_{ij}}$ and $\overline{\rho_{ij}}$ are the average sound velocity and the average density of particles i and j, respectively, as shown in Eqs. (5) and (6) and μ_{ij} is defined as Eq. (7),

$$\overline{c_{ij}}=\frac{(c_i+c_j)}{2}, \quad (5)$$
$$\overline{\rho_{ij}}=\frac{(\rho_i+\rho_j)}{2}, \quad (6)$$
$$\mu_{ij}=\frac{h(U_i^\alpha-U_j^\alpha)(x_i^\alpha-x_j^\alpha)}{(x_i^\beta-x_j^\beta)(x_i^\beta-x_j^\beta)+\varepsilon h^2} \quad (7)$$

Parameters k_1 and k_2 in Eq. (4) are non-dimensional positive constants which determine the effect of artificial viscosity and have an order of 1 (for example $k_1=1.5$ and $k_2=1.5$). The constant ε is a small value (i. e. 0.1) which prevents the denominator from being zero and h is the smoothing length which determines the area of effect of the kernel function. The artificial viscosity Π_{ij} is applied to the stress terms in momentum and energy conservations.

Although numerical divergence is reduced by applying the artificial viscosity in most cases, numerical instability can not be avoided only with the artificial viscosity in some cases. To reduce this high energy in stagnated particles, artificial heat transfer H_i defined as Eq. (8) is added to the energy conservation equation.

$$H_i=2\sum_j\frac{\overline{\zeta_{ij}}}{\overline{\rho_{ij}}}\frac{E_i-E_j}{(x_i^\beta-x_j^\beta)(x_i^\beta-x_j^\beta)}(x_i^\alpha-x_j^\alpha)\,W_{ij,\alpha(i)},$$

(8)

where $\overline{\zeta_{ij}}$ is the average of ζ at particles i and j as shown in Eq. (9),

$$\overline{\zeta_{ij}}=\frac{(\zeta_i+\zeta_j)}{2} \tag{9}$$

The ζ is represented as Eq. (10) where g_1 and g_2 are constants to determine the artificial heat transfer and have the values of order 1.

$$\zeta=g_1 hc+g_2 h^2\left(\left|\frac{\partial U^\alpha}{\partial x^\alpha}\right|-\frac{\partial U^\alpha}{\partial x^\alpha}\right) \tag{10}$$

2.3 Constitutive equation

Total stress tensor $\sigma^{\alpha\beta}$ is expressed in terms of deviatoric stress tensor $S^{\alpha\beta}$ and hydrostatic pressure P as

$$\sigma^{\alpha\beta}=P\delta^{\alpha\beta}+S^{\alpha\beta}, \tag{11}$$

where $\delta^{\alpha\beta}$ is Kronecker's delta. Time derivative of deviatoric stress tensor $\dot{S}^{\alpha\beta}$ is related with deviatoric strain rate tensor $\bar{\dot{\varepsilon}}^{\alpha\beta}$ following the Hooke's law with shear modulus μ for linear elastic behavior as

$$\dot{S}^{\alpha\beta}=2\mu\bar{\dot{\varepsilon}}^{\alpha\beta} \tag{12}$$

Deviatoric strain rate tensor is defined as Eq. (13) where $\dot{\varepsilon}^{\alpha\beta}$ is the strain rate tensor represented as Eq. (14).

$$\bar{\dot{\varepsilon}}^{\alpha\beta}=\left(\dot{\varepsilon}^{\alpha\beta}-\frac{1}{3}\delta^{\alpha\beta}\dot{\varepsilon}^{\gamma\gamma}\right) \tag{13}$$

$$\dot{\varepsilon}^{\alpha\beta}=\frac{1}{2}\left(\frac{\partial U^\alpha}{\partial x^\beta}+\frac{\partial U^\beta}{\partial x^\alpha}\right) \tag{14}$$

The SPH approximation of strain rate tensor is expressed as Eq. (15) from the equation of continuity, Eq. (1).

$$\dot{\varepsilon}^{\alpha\beta}{}_i=\frac{1}{2}\sum_j\frac{m_j}{\rho_i}\{(U_j^\alpha-U_i^\alpha)\,W_{ij,\beta(i)}+(U_j^\beta-U_i^\beta)\,W_{ij,\alpha(i)}\} \tag{15}$$

When the body experiences rotation under constant stress state, the stress variation with time is compensated by Jaumann rate and the time derivative of stress tensor is modified as

$$\dot{S}^{\alpha\beta}-S^{\alpha\gamma}R^{\beta\gamma}-S^{\gamma\beta}R^{\alpha\gamma}=2\mu\bar{\dot{\varepsilon}}^{\alpha\beta}, \tag{16}$$

where the rotation rate tensor $R^{\alpha\beta}$ at a particle i is represented as

$$R_i^{\alpha\beta}=\frac{1}{2}\sum_j\frac{m_j}{\rho_i}\{(U_j^\alpha-U_i^\alpha)\,W_{ij,\beta(i)}-(U_j^\beta-U_i^\beta)\,W_{ij,\alpha(i)}\}. \tag{17}$$

From Eqs. (12)~(16), the time derivative of deviatoric stress can be expressed in the final form as Eq. (18).

$$\dot{S}_i^{\alpha\beta}-S_i^{\alpha\gamma}R_i^{\beta\gamma}-S_i^{\gamma\beta}R_i^{\alpha\gamma}=\mu\sum_j\frac{m_j}{\rho_i}\{(U_j^\alpha-U_i^\alpha)\,W_{ij,\beta(i)}+(U_j^\beta-U_i^\beta)\,W_{ij,\alpha(i)}-\frac{1}{3}\delta^{\alpha\beta}(U_j^\gamma-U_i^\gamma)\,W_{ij,\gamma(i)}\} \tag{18}$$

2.4 Equation of state

Equation of state (EOS) describes relationship between pressure, density, and internal energy of a material. When pressure is not too high, Mie-Grüneisen equation of Eq. (19) can be used to represent the deformation property of metallic materials.

$$P=P_H+\rho\Gamma[E-E_H], \tag{19}$$

where P_H and E_H are the pressure and the internal energy on Hugoniot curve, respectively. Γ is defined as $\Gamma_o\rho_o/\rho$ where Γ_o is Grüneisen parameter and ρ_o is initial density of a particle.

A number of different experimental techniques have been used to measure the response of material to shock wave propagation, where the shock process is considered as irreversible adiabatic process. The most frequently measured parameters are shock wave velocity u_s and particle velocity u_p, and these have the following relationship on the Hugoniot curve.

$$u_s=c_0+s\,u_p, \tag{20}$$

where c_0 and s are parameters for describing waves in a material. Hugoniot internal energy E_H is related with Hugoniot internal pressure P_H as Eq. (21) and P_H can be expressed as Eq. (22) from Eq. (20).

$$E_H=\frac{1}{2}\frac{\eta^*}{\rho_o}P_H, \tag{21}$$

$$P_H=\frac{\rho_0 c_0^2\eta}{(1-s\eta)^2}, \tag{22}$$

where $\eta^*=\rho/\rho_0-1$ and $\eta=1-\rho_0/\rho$. The sound velocity c_s is determined by the definition as

$$c_s{}^2=\left(\frac{\partial P}{\partial\rho}\right) \tag{23}$$

3. Searching Algorithm and Time Integration

In order to search neighbor particles, linked-list searching algorithm is adopted. Box-type grids are applied to the problem domain and the particle positions are determined in the domain. The relative positions and distances between particles are computed. Those particles within specific smoothing length of a particle are included in computing the influences which are to be given on the particle.

Particles are getting close or disperse during deformation process. Computing time increases when particles approach each other and particles within the search radius consequently increase. On the other hand, relations between adjacent particles are disconnected if the particles are dispersed. A variable smoothing length is adopted in order to overcome these difficulties. The time variation of smoothing length is expressed as

$$\left(\frac{dh}{dt}\right)_i=-\left(\frac{h_i}{N_D\rho_i}\right)\rho_i\sum_j\frac{m_j}{\rho_i}(U_i^\beta-U_j^\beta)\,W_{ij,\beta}, \tag{24}$$

where N_D represents dimension and has values of 1, 2, or 3.

Time derivatives of density, velocity, and energy determined by the continuity equation, momentum conservation equation, and energy conservation equation are integrated with respect to time. The time integration of density, energy, and smoothing length can be written as

$$\rho_i^{n+1}=\rho_i^n+\delta t^n\left(\frac{d\rho}{dt}\right)_i \tag{25}$$

$$E_i^{n+1}=E_i^n+\delta t^n\left(\frac{dE}{dt}\right)_i \tag{26}$$

$$h_i^{n+1}=h_i^n+\delta t^n\left(\frac{dh}{dt}\right)_i \tag{27}$$

where superscripts n and $n+1$ represent the time instants t and $t+\delta t$, respectively. The velocity of a particle is obtained at the middle of time t and $t+\delta t$ for application of central difference.

$$U_i^{n+\frac{1}{2}}=U_i^{n-\frac{1}{2}}+\frac{1}{2}(\delta t^n+\delta t^{n-1})\left(\frac{dU}{dt}\right)_i \tag{28}$$

where superscripts $n-{}^1/_2$ and $n+{}^1/_2$ represent the time instants $t-{}^1/_2\delta t^{n-1}$ and $t+{}^1/_2\delta t^n$, respectively. The position of a particle at time instant $t+\delta t$ can be written as

$$x_i^{n+1}=x_i^n+\delta t^n U_i^{n+1/2} \tag{29}$$

The above density, energy, smoothing length, and position of a particle are forwarded to the computations at the next step and this process of time integration is repeated.

4. Contact Algorithm

4.1 The characteristics of SPH at contact surface

In the SPH, the field variables at an arbitrary particle are calculated through interpolations on adjacent particles with a kernel function. When two material bodies approach each other and are engaged in contact, particles in the different bodies start to exert influences mutually near the contact surface.

In contrast to other hydrocodes based on grids, the boundary surface of a body is relatively obscure in the SPH so that exact determination of contact surface is considerably difficult. It is also difficult to determine whether the contact is achieved, because it is possible that particles start interacting even if those are in different bodies and contact is not established. Also required is relevant treatment of interaction on the contact interface between two bodies when the contact is established. Although only velocity components normal to the contact surface should be considered in the calculation of interaction, the field variables of a particle are affected by tangential components of particles in the opposite body. This situation produces artificial friction at contact surface. In case of separation after the contact, the interaction between particles in different bodies persist while the particles should have no influence on each other. This is also due to the concept of interpolation by kernel function using smoothing length. This situation results in artificial tension where the particles at contact surface are in cluster.

In analysis of elasto-plastic deformation under low velocity impact, the treatment of contact

condition will produce considerable effect on the analysis, even though the effect can be neglected on high velocity impact which involves large deformation in transient time. A contact algorithm is proposed and utilized to resolve the undesirable effects at contact surface. This algorithm is based on the non-mass artificial particles located at contact surface and the contact criterion which are introduced in the followings.

4.2 Non-mass artificial particle

The SPH particle approximation of field variables at particle i to be calculated in continuity equation, momentum and energy conservation equations, is a function of mass at particle j only, as shown in Eqs. (1) ~ (3). Hence when the mass of a particle j is assumed to be zero, the field variables at a particle i can be calculated from the other real particle j which has its own values of field variables without receiving the effect from the non-mass particle. On the contrary, the field variables of non-mass particle can be calculated through the interpolation on real particles, as usual.

The non-mass artificial particle can be utilized as boundary particle for the material body to be simulated. In this case the shape of a material body can be exactly presented and the normal unit direction vector at boundary particle can be presented in order to specify the boundary characteristics. The position of real and artificial particles, and the concept of normal vector are illustrated in Fig. 1. Real particles are located inside a material body and artificial particles are located on the boundary of material body in order to represent the boundary surface and specify the normal vector to the surface.

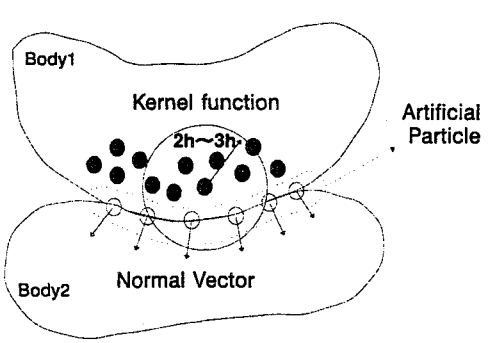

Fig. 1 Concept of artificial particle and normal vector on boundary surface

The normal unit direction vector of artificial particle is changed with a time step through the application of the rotation rate tensor defined in Eq. (17) which is calculated at the non-mass artificial particle. The normal unit direction vector of a real particle in a material body can be obtained with a normalization of the normal vector of artificial particles interpolated by a kernel function as

$$\boldsymbol{n}_i=\frac{\sum_k \boldsymbol{n}_k W_{ik}}{\left|\sum_k \boldsymbol{n}_k W_{ik}\right|} \tag{30}$$

where $\boldsymbol{n}_i$ is normal unit direction vector of real particle i, $\boldsymbol{n}_k$ is the normal unit direction vector of an artificial particle k, and W_{ik} is kernel function between real particle i and artificial particle k.

4.3 Contact Criterion

Since the initiation of contact can be defined when the particles near contact surface approach each other in the normal direction to the contact surface, the velocity of particles shall be projected on the normal direction to the contact surface. When the normal unit direction vectors of particles in two impacting material bodies represents a difference, an average value shall be calculated for the common normal unit direction vector of particles under interaction. With consideration of the particle velocities projected to normal direction and the relative position between particles, the contact criterion can be represented as

$$(U_i^\alpha - U_j^\alpha)^* \cdot (x_i^\alpha - x_j^\alpha) < 0 \tag{31}$$

where $(U_i^\alpha - U_j^\alpha)^*$ means the difference between the projected velocity of particles i and j. If an interaction between the particles from different material bodies satisfy Eq. (31), the contact situation is assumed. When Eq. (31) is not satisfied, the interaction between two particles is eliminated. For a particle i to be calculated, the velocity difference for the interaction with particle j is considered in the calculation, where the other particles in a material body, of the same material

with the particle i, is interpolated with kernel function, as usual. Since the proposed contact algorithm is based on non-mass artificial particles initially located at boundary surface, its application may be limited to the simulation of transient elasto-plastic deformation without fracture. As a sample calculation for the investigation on the characteristics of contact algorithm, a simulation of the axial impact of two elastic rods is performed with and without contact algorithm.

5. Axial Impact of Two Elastic Rods

5.1 Simulation conditions

The wave propagation in elastic rods which are axially colliding, is simulated with SPH. An iron rod of length L=20 mm and radius R=1 mm impacts at a velocity of V=50 m/s axially on a rod at rest of the same material and dimension. Kernel function used in the simulation is cubic B-spline type (Libersky et al., 1993) where the initial smoothing length h is 0.1 mm and the number of particles per smoothing length is 1.0. Monaghan and Gingold's artificial viscosity (1983, 1988) is used for the numerical stability of shock where $\alpha=1.0$ and $\beta=1.0$. Since the impact situation in this paper is relatively low velocity impact, the artificial heat transfer is not included in the simulation. Material behavior under the impact is described by linear elastic constitutive equation and Mie-Gr neisen equation of state where the values of parameters for iron are listed in Table 1.

Table 1 Elastic and Mie-Grüneisen parameters of iron

Parameter	Symbol	Value
Elastic modulus	E_0	189.6 GPa
Shear modulus	μ	80.0 GPa
Density	ρ_0	7.85 g/cm^3
Sound velocity	c_0	3.574 km/s
Particle velocity factor	s	1.92
Mie-Grüneisen parameter	Γ_0	1.69

5.2 Simulation results

In this numerical experiment, compressive wave due to the impact is traveling from the contact surface toward the free ends of the two rods. Once the compression waves reach at the free ends, tension waves will be produced and travel backward to the contact surface. The impacting surface will remain in contact until the propagated waves return as a tensile wave. At this moment, the impacting rod will be at rest and the impacted rod will move away at the velocity of impacting rod.

The behavior of particles in the elastic two rods before the impact and after the separation of contact surface is shown in Figs. 2 and 3 for the simulation without and with the contact algorithm, respectively. The simulation by traditional SPH formulation, as shown in Fig. 2, represents that the particles in two rods near the contact

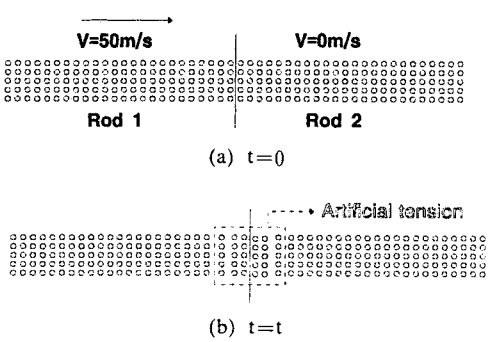

Fig. 2 The behavior of particles in elastic two rods before impact and after the separation of contact surface without contact algorithm

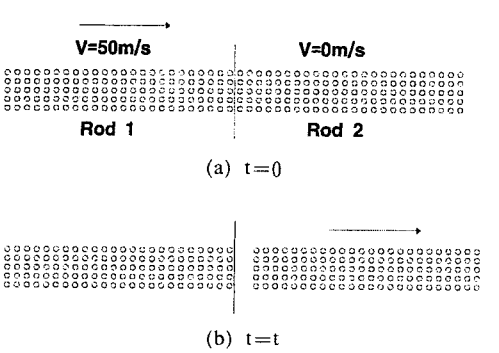

Fig. 3 The behavior of particles in elastic two rods before impact and after the separation of contact surface with contact algorithm

surface are in a cluster and the exact transfer of kinetic energy between two rods are prohibited. This is an artificial tension originated from the basic concept of the SPH where the field variable and spatial derivative of particle are determined from the interpolation of the adjacent particles. When the simulation is performed with the consideration of a proposed contact algorithm as shown in Fig. 3, the artificial tension disappears and the transfer of kinetic energy is fulfilled in that the impacting rod is at rest and the impacted rod moves away with the velocity of impacting rod.

For the detailed analysis of the elastic wave propagation and kinetic energy transfer, the particle velocity profile in the two impacting rods is illustrated in Fig. 4 at 5 instants; (a) 0 μs, (b) 3 μs, (c) 6 μs, (d) 9 μs, and (e) 12 μs. In Fig. 4,

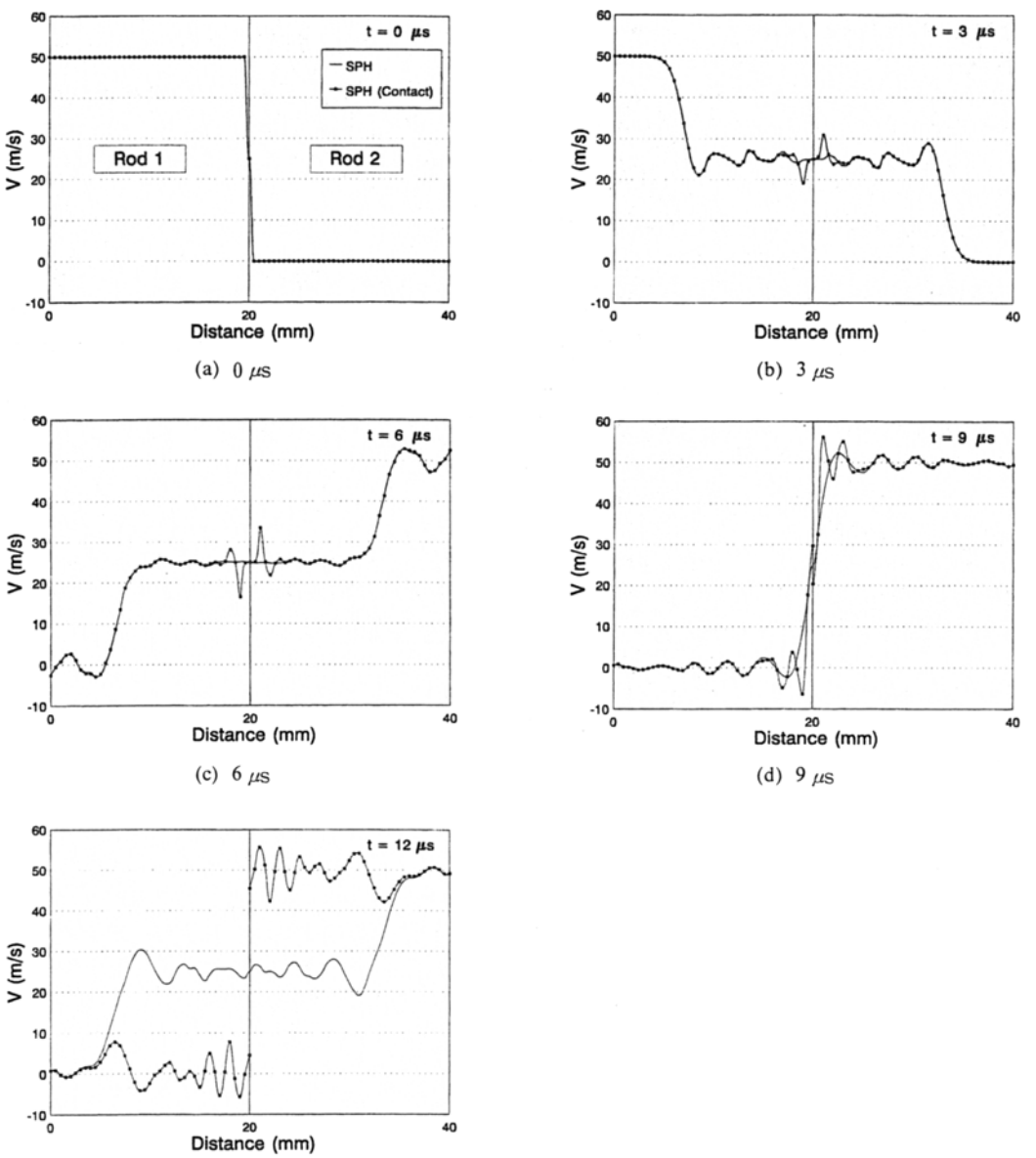

Fig. 4 Particle velocity profiles in elastic impact rods without or with the contact algorithm

the distance represents the sum of the length of two rods which is 40 mm and the contact surface is located at the distance of 20 mm. There are two curves in each illustration of Fig. 4, the curves of solid line represent the SPH results without the contact algorithm, while the curves with dots show the results with the contact algorithm.

On the instant of contact, shown in Fig. 4(a), the velocities of the impacting rod and the impacted rod are 50 m/s and 0 m/s, respectively. In Fig. 4(b) showing the particle velocities at 3μs after the impact, the compression waves travel toward the end of each rods and the particle velocities in the rods propagated by compression waves are shown as 25 m/s. The compression waves will reach the free ends and return as tension waves. A zero particle velocity near the free end of the impacting rod is shown in Fig. 4 (c). On the other hand, the free end of the impacted rod has the particle velocity of 50 m/s. The particle velocity near the contact surface remains at 25 m/s. In Fig. 4(d) showing the particle velocities at 9 μs, the two rods are separated. The particle velocity of the impacting rod is approximately zero while that of the impacted rod is approximately 50 m/s. Up to this time, the results without and with the contact algorithm do not represent any difference. However the particle velocity profiles after the initiation of separation due to the arrival of tension wave on contact surface, shown in Fig. 4(e), represent the difference. Without contact algorithm, the particles near the contact surface are in a cluster and the particles in both rods move with same velocity. Meanwhile with contact algorithm, since the particles in both rods have no connection each other if the contact criterion is not satisfied, the impacting rod is at rest and the impacted rod moves away with the velocity of impacting rod.

5.3 Comparison with a theoretical analysis

In one-dimensional elastic wave propagation theory, the kinetic energy of the impacting material is exactly transferred to the impacted material. The moving velocity of the impacted rod will be the velocity of the impacting rod. The elastic

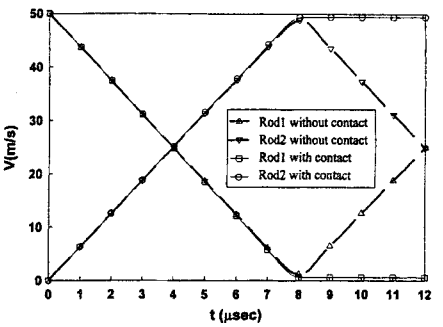

Fig. 5 The SPH simulation result on the average velocities of two impact rods

wave velocity C_L in a rod can be expressed as a function of elastic modulus E_0 and initial material density ρ_o.

$$C_L=\sqrt{\frac{E_0}{\rho_0}} \tag{32}$$

In the present simulation, the calculated elastic wave velocity is 4914.6 m/s by using the material data in Table 1. The contact duration for the rods having same dimension and material will be given by Eq. (33) where t is the contact duration, L is the length of rod, and C_L is defined as Eq. (32).

$$t=2\ L/C_L \tag{33}$$

The contact duration in the present simulation is given as 8.14μs. The SPH simulation result on the variation of the rod velocity averaged by using the particle velocities in the impacting rod or the impacted rod is presented in Fig. 5. The curves with the dashed line represent the velocity without the contact algorithm while the curves with solid line show the velocity with contact algorithm.

In both cases until the approximately 8 μs the velocity of the impacting rod is linearly decreasing and becomes about 0.3 m/s. On the other hand, the velocity of the impacted rod is linearly increasing and becomes about 49.7m/s which is approximately the velocity of impacting rod. These results by SPH are considerably close to the results of theoretical analysis based on one dimensional elastic wave propagation theory.

After the initiation of separation, even though the simulation result using contact algorithm represents the constant velocity, the simulation result using no contact algorithm represents the

reduction of velocity which has no physical meaning.

6. Conclusion

Elastic wave propagation by the low velocity impact of two rods is analysed by SPH which is a gridless pure Lagrangian hydrocode. A tension instability on the contact surface is shown in the simulation based on the SPH formulation. Artificial particles on the boundary of material body, especially on the contact surface of low velocity impact, are introduced in order to alleviate the effect of kernel function between the departing bodies. A contact algorithm, based on the non-mass artificial particles located at the contact surface, is proposed to resolve the problem due to the artificial tension and friction.

The behavior of the low velocity axial impact of two rods with the proposed contact algorithm is simulated and consistent with the theory based on elastic wave propagation. The inconsistency between the elastic wave theory and simulation without the contact algorithm shows the effect of the contact algorithm.

Even though the contact algorithm proposed in this paper has been investigated in elastic deformation, it can be applied to the analysis of transient elasto-plastic deformation except the phenomenon involving fracture or fragmentation.

Acknowledgement

This study is supported by the academic research fund (ME97-C-23) of Ministry of Education, Republic of Korea. The support is greatly appreciated.

References

Gingold, R. A. and Monaghan, J. J., 1977, "Smoothed Particle Hydrodynamics: Theory and Applications to Non-Spherical Stars," *Mon. Not. R. Astron. Soc.*, Vol. 181, pp. 375~389.

Gingold, R. A. and Monaghan, J. J., 1982, "Kernel Estimates as a Basis for General Particle Methods in Hydrodynamics," *J. Comp. Phys.*, Vol. 46, pp. 429~453.

Libersky, L. D. and Petschek, A. G., 1990, "Smoothed Particle Hydrodynamics with Strength of Materials," *Advances in the Free-Lagrange Method, Lecture Notes in Physics*.

Libersky, L. D., Petschek, A. G., Carney, T. C., Hipp, J. R. and Allahdadi, F. A., 1993, "High Strain Lagrangian Hydrodynamics: A Three -Dimensional SPH Code for Dynamic Material Response," *J. Comp. Phys.*, Vol. 109, pp. 67~75.

Lucy, L. B., 1977, "A Numerical Approach to the Testing of the Fission Hypothesis," *Astron. J.*, Vol. 82, pp. 1013~1020.

Monaghan, J. J. and Gingold, R. A., 1983, "Shock Simulation by the Particle Method SPH," *J. Comp. Phys.*, Vol. 52, pp. 374~389.

Monaghan, J. J., 1988, "An Introduction to SPH," *Comp. Phys. Comm.*, Vol. 48, pp. 89~96.

Monaghan, J. J., 1992, "Smoothed Particle Hydrodynamics," *Annu. Rev. Astron. Astrophys.*, Vol. 30, pp. 543~574.

Appendix

A.1 Kernel function and particle approximation

Function $f(\boldsymbol{r}_0)$ at point $\boldsymbol{r}_0$ can be expressed as an integration of the product of $f(\boldsymbol{r})$ and Dirac delta function $\delta(\boldsymbol{r}_0-\boldsymbol{r})$

$$f(\boldsymbol{r}_0)=\int_\Omega f(\boldsymbol{r})\,\delta(\boldsymbol{r}_0-\boldsymbol{r})\,d\boldsymbol{r} \tag{A1}$$

Kernel approximation $\langle f(\boldsymbol{r}_0)\rangle$ of function $f(\boldsymbol{r}_0)$ is defined as

$$\langle f(\boldsymbol{r}_0)\rangle=\int_\Omega f(\boldsymbol{r})\,W(\boldsymbol{r}_0-\boldsymbol{r},\,h)\,d\boldsymbol{r} \tag{A2}$$

where $W(\boldsymbol{r}_0-\boldsymbol{r},\,h)$ is a kernel function and h is a smoothing length. The kernel function should satisfy the condition $W\rightarrow\delta$ to resemble the Dirac delta function as $h\rightarrow 0$. This requires

$$\int_\Omega W(\boldsymbol{r}_0-\boldsymbol{r},\,h)\,d\boldsymbol{r}=1 \text{ as } h\rightarrow 0 \tag{A3}$$

The particle approximation converted from the kernel approximation can be written as Eq. (A4) using the concept of unit volume with mass m and density ρ.

$$f(\boldsymbol{r})_i=\sum_{j=1}^{n}\frac{m_j}{\rho_j}f(\boldsymbol{r}_j)\,W(\boldsymbol{r}_i-\boldsymbol{r}_j,\,h) \qquad \text{(A4)}$$

The function at particle i is determined from the interpolation of function at neighbouring particle j by the kernel function.

A.2 SPH approximation of differential equations

When a function F is given as the multiplication of a function F_1 and a derivative in the direction x^a of function F_2 as Eq. (A5),

$$F=F_1\frac{\partial F_2}{\partial x^a} \qquad \text{(A5)}$$

the kernel approximation of the function F at particle i can be expressed as Eq. (A6) by using Eq. (A2).

$$\begin{aligned}\langle F_i\rangle&=\int F_{1j}\frac{\partial F_{2j}}{\partial x_j^a}W_{ij}dx_j \qquad \text{(A6)}\\ &=F_{1i}\int\frac{\partial F_{2j}}{\partial x_j^a}W_{ij}dx_j\\ &\quad+\int(F_{1j}-F_{1i})\frac{\partial F_{2j}}{\partial x_j^a}W_{ij}dx_j\end{aligned}$$

W_{ij} represents a kernel function $W(x_i-x_j,\,h)$ between particles i and j. When the variation of F_1 between particle i and particle j is negligible, the kernel approximation of the function F at particle i becomes

$$\langle F_i\rangle=F_{1i}\int\frac{\partial F_{2j}}{\partial x_j^a}W_{ij}dx_j \qquad \text{(A7)}$$

With the integration by part and the condition that the kernel function on the boundary of integration is zero, the Eq. (A7) becomes the Eq. (A8) in its simple form.

$$\langle F_i\rangle=-F_{1i}\int F_{2j}\frac{\partial W_{ij}}{\partial x_j^a}dx_j \qquad \text{(A8)}$$

The particle approximation of this function becomes Eq. (A9) from the concept of Eq. (A4).

$$F_i=-F_{1i}\sum_j\frac{m_j}{\rho_i}F_{2j}W_{ij,a(j)} \qquad \text{(A9)}$$

where $W_{ij,a(j)}$ represents the derivative of kernel function W_{ij} with respect to coordinate x_j^a. When the kernel function is an even function, the derivative of kernel function with respect to coordinate x_j^a can be replaced by the derivative with respect to coordinate x_i^a

$$F_i=F_{1i}\sum_j\frac{m_j}{\rho_j}F_{2j}W_{ij,a(i)} \qquad \text{(A10)}$$

Even though the particle approximation of Eq. (A10) is the simplest method to have the form of SPH approximation, its use represents difficulties in the practical application to the analysis of hydrodynamic problems. Hence the various other approximation equations, based on and modifying the concept of Eq. (A10), has been developed. One of these method, the usual method is that the function F is transformed into an another form like as Eq. (A11) and then each item follow the basic SPH approximation.

$$F=F_1\frac{\partial F_2}{\partial x^a}=\frac{\partial(F_1F_2)}{\partial x^a}-F_2\frac{\partial F_1}{\partial x^a} \qquad \text{(A11)}$$